

Charmonium-nucleon potential from lattice QCD

Taichi Kawanai* and Shoichi Sasaki†

*Department of Physics, The University of Tokyo,
Hongo 7-3-1, Tokyo 113-0033, Japan*

(Dated: November 5, 2018)

We present results for the charmonium-nucleon potential $V_{c\bar{c}-N}(r)$ from quenched lattice QCD, which is calculated from the equal-time Bethe-Salpeter amplitude through the effective Schrödinger equation. Detailed information of the low-energy interaction between the nucleon and charmonia (η_c and J/ψ) is indispensable for exploring the formation of charmonium bound to nuclei. Our simulations are performed at a lattice cutoff of $1/a \approx 2.1$ GeV in a spatial volume of $(3 \text{ fm})^3$ with the nonperturbatively $\mathcal{O}(a)$ improved Wilson action for the light quarks and a relativistic heavy quark action for the charm quark. We have found that the potential $V_{c\bar{c}-N}(r)$ for either the η_c and J/ψ states is weakly attractive at short distances and exponentially screened at large distances. The spin averaged J/ψ - N potential is slightly more attractive than that of the η_c - N case.

Heavy quarkonium states such as charmonium ($c\bar{c}$) states do not share the same quark flavor with the nucleon (N). This suggests that the heavy quarkonium-nucleon interaction is mainly induced by the genuine QCD effect of multi-gluon exchange [1–3]. Therefore the $c\bar{c}$ - N system is ideal to study the effect of multi-gluon exchange between hadrons. As an analog of the van der Waals force, the simple two-gluon exchange contribution gives a weakly attractive, but long-ranged interaction between the heavy quarkonium state and the nucleon [4, 5]. However, the validity of calculations based on a perturbative theory is questionable for QCD where the strong interaction influences the long distance region.

The $c\bar{c}$ - N scattering at low energy has been studied from first principles of QCD. The s -wave J/ψ - N scattering length is about 0.1 fm by using QCD sum rules [6] and 0.71 ± 0.48 fm (0.70 ± 0.66 fm for η_c - N) by lattice QCD [7], while it is estimated as large as 0.25 fm from the gluonic van der Waals interaction [2]. All studies suggest that the $c\bar{c}$ - N interaction is weakly attractive. This indicates that the formation of charmonium bound to nuclei is enhanced. In 1991, Brodsky *et al.* had argued that the $c\bar{c}$ -nucleus (A) bound system may be realized for the mass number $A \geq 3$ if the attraction between the charmonium and the nucleon is sufficiently strong [1, 8]. Therefore, precise information on the $c\bar{c}$ - N potential $V_{c\bar{c}-N}(r)$ is indispensable for exploring nuclear-bound charmonium states like the η_c - ^3He or J/ψ - ^3He bound state in few body calculations [9].

We recall the recent great success of the N - N potential from lattice QCD [10]. In this new approach, the potential between hadrons can be calculated from the equal-time Bethe-Salpeter (BS) amplitude through an effective Schrödinger equation. Thus, direct measurement of the $c\bar{c}$ - N potential is now feasible by using lattice QCD. It should be important to give a firm theoretical prediction about the nuclear-bound charmonium, which is possibly investigated by experiments at J-PARC and FAIR/GSI.

The method utilized here to calculate the hadron-hadron potential in lattice QCD is based on the same

idea originally applied for the N - N potential [10, 11]. We first calculate the equal-time BS amplitude of two local operators (hadrons h_1 and h_2) separated by given spatial distances ($r = |\mathbf{r}|$) from the following four-point correlation function:

$$G^{h_1-h_2}(\mathbf{r}, t; t_2, t_1) = \sum_{\mathbf{x}} \sum_{\mathbf{x}', \mathbf{y}'} \langle h_1(\mathbf{x}, t) h_2(\mathbf{x} + \mathbf{r}, t) (h_1(\mathbf{x}', t_2) h_2(\mathbf{y}', t_1))^\dagger \rangle,$$

where \mathbf{r} is the relative coordinate of two hadrons at sink position (t). Each hadron operator at source positions (t_1 and t_2) is separately projected onto a zero-momentum state by a summation over all spatial coordinates \mathbf{x}' and \mathbf{y}' . To avoid the Fierz rearrangement of two-hadron operators, it is better to set $t_2 \neq t_1$. Without loss of generality, we choose $t_2 = t_1 + 1 = t_{\text{src}}$ hereafter. Suppose that $|t - t_{\text{src}}| \gg 1$ is satisfied, the correlation function asymptotically behaves as

$$G^{h_1-h_2}(\mathbf{r}, t; t_{\text{src}}) \propto \phi_{h_1-h_2}(\mathbf{r}) e^{-E_{h_1-h_2}(t-t_{\text{src}})}, \quad (1)$$

where the \mathbf{r} -dependent amplitude, which is defined as

$$\phi_{h_1-h_2}(\mathbf{r}) = \sum_{\mathbf{x}} \langle 0 | h_1(\mathbf{x}) h_2(\mathbf{x} + \mathbf{r}) | h_1 h_2; E_{h_1-h_2} \rangle \quad (2)$$

with the total energy $E_{h_1-h_2}$ for the ground state of the two-particle h_1 - h_2 state, corresponds to a part of the equal-time BS amplitude and is called the BS wave function [12, 13]. After an appropriate projection with respect to discrete rotation

$$\phi_{h_1-h_2}^{A_1^+}(r) = \frac{1}{24} \sum_{\mathcal{R} \in O_h} \phi_{h_1-h_2}(\mathcal{R}^{-1}\mathbf{r}), \quad (3)$$

where \mathcal{R} represents 24 elements of the cubic group O_h , one can get the BS wave function projected in the A_1^+ representation, which corresponds to the s -wave in continuum theory at low energy. Once the BS wave functions $\phi_{h_1-h_2}^{A_1^+}(r)$ are calculated in lattice simulations, the

TABLE I: Simulation parameters in this study. The Sommer parameter $r_0 = 0.5$ fm is used to fix the scale [14, 15].

| | a | a^{-1} | Lattice size | $\sim La$ | |
|---------|--------|----------|------------------|-----------|------------|
| β | [fm] | [GeV] | $(L^3 \times T)$ | [fm] | Statistics |
| 6.0 | 0.0931 | 2.12 | $16^3 \times 48$ | 1.5 | 200 |
| | | | $32^3 \times 48$ | 3.0 | 602 |

hadron-hadron “effective” central potential with the energy eigenvalue E of the stationary Schrödinger equation, can be obtained by

$$V_{h_1-h_2}(r) - E = \frac{1}{2\mu} \frac{\nabla^2 \phi_{h_1-h_2}^{A^+}(r)}{\phi_{h_1-h_2}^{A^+}(r)}, \quad (4)$$

where μ is the reduced mass of the h_1 - h_2 system and ∇^2 is defined by the discrete Laplacian with nearest-neighbor points. Although the energy eigenvalue E is supposed to be the energy difference between the total energy of two hadrons ($E_{h_1-h_2}$) and the sum of the rest mass of individual hadrons ($M_{h_1} + M_{h_2}$), we instead determine E with the condition of $\lim_{r \rightarrow \infty} \{V_{h_1-h_2}(r) - E\} = 0$ [13]. More details of this method can be found in Ref. [11].

Let us first consider the low energy η_c - N interaction, which does not possess a spin-dependent part. We use the conventional interpolating operators, $h_1(x) = \epsilon_{abc}(u_a(x)C\gamma_5 d_b(x))u_c(x)$ for the nucleon and $h_2(y) = \bar{c}_a(y)\gamma_5 c_a(y)$ for the η_c state, where a, b and c are color indices, and $C = \gamma_4\gamma_2$ is the charge conjugation matrix. We have performed quenched lattice QCD simulations on two different lattice sizes, $L^3 \times T = 32^3 \times 48$ and $16^3 \times 48$, with the single plaquette gauge action at $\beta = 6/g^2 = 6.0$, which corresponds to a lattice cutoff of $a^{-1} \approx 2.1$ GeV according to the Sommer scale [14, 15]. Our main results are obtained from the data taken on the larger lattice ($La \approx 3.0$ fm). A supplementary data with a smaller lattice size ($La \approx 1.5$ fm) are used for a test of finite-size effects. The number of statistics is $\mathcal{O}(600)$ for $L = 32$ and $\mathcal{O}(200)$ for $L = 16$, respectively. The simulation parameters and the number of sampled gauge configurations are summarized in Table I.

We use non-perturbatively $\mathcal{O}(a)$ improved Wilson fermions for light quarks (q) [16] and a relativistic heavy quark (RHQ) action for the charm quark (Q) [17]. The RHQ action is a variant of the Fermilab approach [18], which can remove large discretization errors for heavy quarks. The hopping parameter is chosen to be $\kappa_q = 0.1342, 0.1339, 0.1333$, which correspond to $M_\pi = 0.64, 0.72, 0.87$ GeV ($M_N = 1.43, 1.52, 1.70$ GeV), and $\kappa_Q = 0.1019$ which is reserved for the charm-quark mass ($M_{\eta_c} = 2.92$ GeV and $M_{J/\psi} = 3.00$ GeV) [19]. Each hadron mass is obtained by fitting the corresponding two-point correlation function with a single exponential form. We calculate quark propagators with wall sources, which are located at $t_{\text{src}} = 5$ for the light quarks and

at $t_{\text{src}} = 4$ for the charm quark, with Coulomb gauge fixing. It is worth mentioning that Dirichlet boundary conditions are imposed for quarks in the time direction in order to avoid wrap-round effects, which are very cumbersome in systems of more than two hadrons [20]. In addition, the ground state dominance in four-point functions is checked by an effective mass plot of total energies of the $c\bar{c}$ - N system.

The left panel of Fig. 1 shows a typical result of the projected BS wave function at the smallest quark mass, which is evaluated by a weighted average of data in the time-slice range of $16 \leq t - t_{\text{src}} \leq 35$. The wave functions are normalized to unity at a reference point $\mathbf{r} = (16, 16, 16)$, which is supposed to be outside of the interaction region. As shown in Fig. 1, the wave function is enhanced from unity near the origin so that the low-energy η_c - N interaction is certainly attractive. This attractive interaction, however, is not strong enough to form a bound state as is evident from this figure, where the wave function is not localized, but extends to large distances.

In the right panel of Fig. 1, we show the effective central η_c - N potential, which is evaluated by the wave function through Eq. (4) with measured values of E and μ . As is expected, the η_c - N potential clearly exhibits an entirely attractive interaction between the charmonium and the nucleon without any repulsion at either short or large distances. The short range attraction is deemed to be a result of the absence of Pauli blocking, that is a relevant feature in this particular system of the heavy quarkonium and the light hadron. The interaction is exponentially screened in the long distance region $r \gtrsim 1$ fm [25]. This is consistent with the expected behavior of the color van der Waals force in QCD, where the strong confining nature of color electric fields must emerge [5, 21]. The exponential-type damping in the color van der Waals force is hardly introduced by any perturbative arguments.

In detail, a long-range screening of the color van der Waals force is confirmed by the following analysis. We have tried to fit data with two types of fitting functions: i) exponential type functions $-\exp(-r^m)/r^n$, which include the Yukawa form ($m = 1$ and $n = 1$), and ii) inverse power law functions $-1/r^m$, where n and m are not restricted to be integers. The former case can easily accommodate a good fit with a small χ^2/ndf value, while in the latter case we cannot get any reasonable fit. For example, the functional forms $-\exp(-r)/r$ and $-1/r^7$ give $\chi^2/\text{ndf} \simeq 2.5$ and 34.3 , respectively. It is clear that the long range force induced by a normal “van der Waals” type interaction based on two-gluon exchange [5] is non-perturbatively screened.

If we adopt the Yukawa form $-\gamma e^{-\alpha r}/r$ to fit our data of $V_{c\bar{c}-N}(r)$, we obtain $\gamma \sim 0.1$ and $\alpha \sim 0.6$ GeV. These values should be compared with the phenomenological $c\bar{c}$ - N potential adopted in Refs. [1], where the parameters ($\gamma = 0.6, \alpha = 0.6$ GeV) are barely fixed by a Pomeron

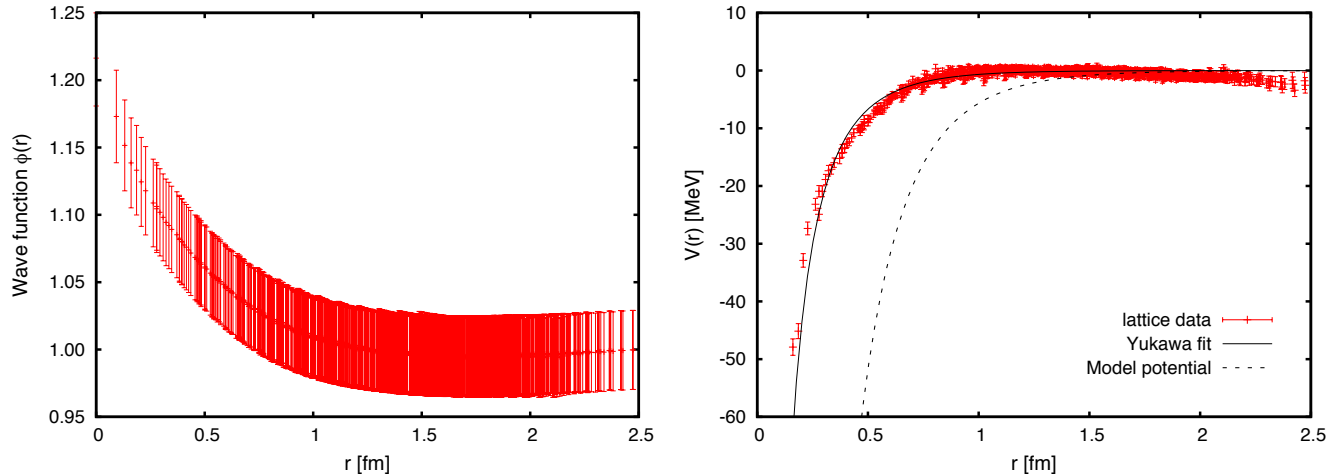


FIG. 1: The wave function (left) and the effective central potential (right) in the s -wave η_c - N system for $M_\pi = 0.64$ GeV as a typical example. In the right panel we fit a Yukawa potential (solid line) and compare with the phenomenological potential (dashed) adopted in Ref. [1].

exchange model. The strength of the Yukawa potential γ is six times smaller than the phenomenological value, while the Yukawa screening parameter α obtained from our data is comparable. The $c\bar{c}$ - N potential obtained from lattice QCD is rather weak.

We next show both finite-size and quark-mass dependence of the η_c - N potential in Fig. 2. Firstly, as shown in the left panel of Fig. 2, there is no significant difference between potentials computed from lattices with two different spatial sizes ($La \approx 3.0$ and 1.5 fm). This observation is simply due to the fact that the η_c - N potential is quickly screened to zero and turns out to be somehow short ranged. In principle, the short range part of the potential, which is represented by ultraviolet physics, should be insensitive to the spatial extent associated with an infrared cutoff. As a result, it is assured that the larger lattice size is large enough to study the η_c - N system.

No large quark-mass dependence is also observed in the right panel of Fig. 2. This is a non-trivial feature since there is an explicit dependence on the reduced mass μ in the definition of the effective central potential (4). However, if one recalls that the $c\bar{c}$ - N interaction is mainly governed by multi-gluon exchange, the resulting potential is expected to be less sensitive to the reduced mass of the considered system ignoring the internal structures of the η_c and nucleon states.

If one takes a closer look at the inset of Figure 2, it is found that the nature of the attractive interaction in the η_c - N system tends to get slightly weaker as the light quark mass decreases. Does this mean that the strength of the η_c - N potential at the physical point becomes much weaker than what we measured at the quark mass simulated in this study? The answer to this question is not simple. It is worth to remember that the ordinary van der

Waals interaction is sensitive to the size of the charge distribution, which is associated to the dipole size. Larger dipole size yields stronger interaction. We may expect that the size of the nucleon becomes large as the light quark mass decreases. However, the very mild but opposite quark-mass dependence observed here does not accommodate this expectation properly.

Recent detailed studies of nucleon form factors tell us that the root mean-square (rms) radius of the nucleon, which is a typical size of the nucleon, shows rather mild quark-mass dependence and its value is much smaller than the experimental value up to at $M_\pi \sim 0.3$ GeV (for example, see [23]). At the chiral limit in baryon chiral perturbation theory the rms radius is expected to diverge logarithmically [24]. This implies that the size of the nucleon increases drastically in the vicinity of the physical point. It may be phenomenologically regarded as the “pion-cloud” effect. We notice here that our simulations are performed in the quenched approximation and at rather heavy quark masses. We speculate that the $c\bar{c}$ - N potential from dynamical simulations would become more strongly attractive in the vicinity of the physical point, where the size of the nucleon is much larger than at the quark mass simulated in this study.

We also have calculated the J/ψ - N potential. It should be noted here that different total spin states are allowed as spin-1/2 and spin-3/2 states in the J/ψ - N system. This fact introduces a little complexity regarding the spin-dependence on the J/ψ - N potential. The interpolating operator of the J/ψ state is defined as $h_{2,i}(y) = \bar{c}_a(y)\gamma_i c_a(y)$, which carries the specific spin polarization direction. Therefore, the four-point correlation function for the J/ψ - N state becomes a matrix form with spatial Lorentz indices, $G_{ij}^{h_1-h_2} = \langle h_1 h_{2,i}(h_1 h_{2,j})^\dagger \rangle$.

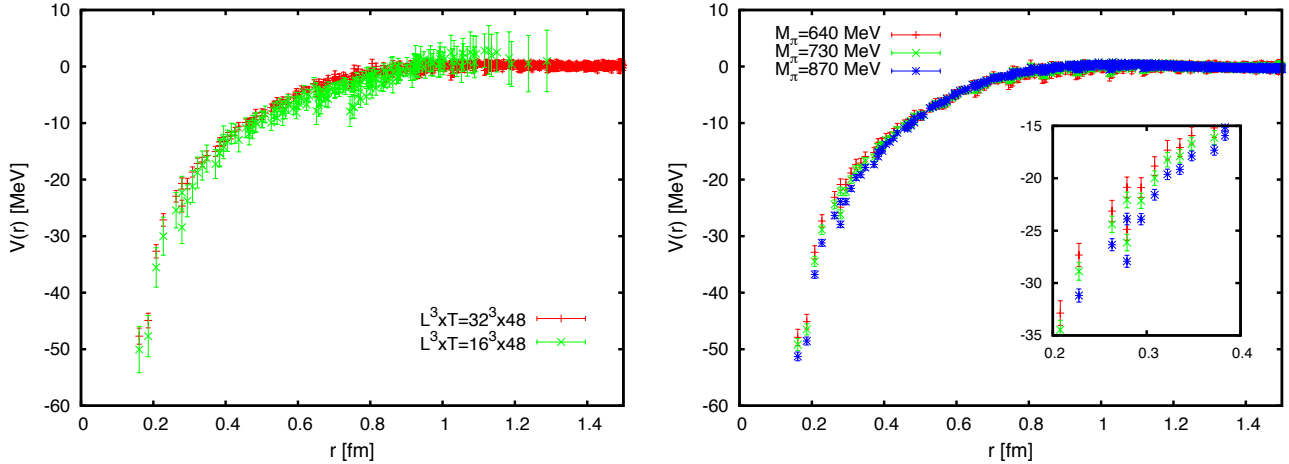


FIG. 2: The volume dependence (left) and the quark-mass dependence (right) of the η_c - N potential.

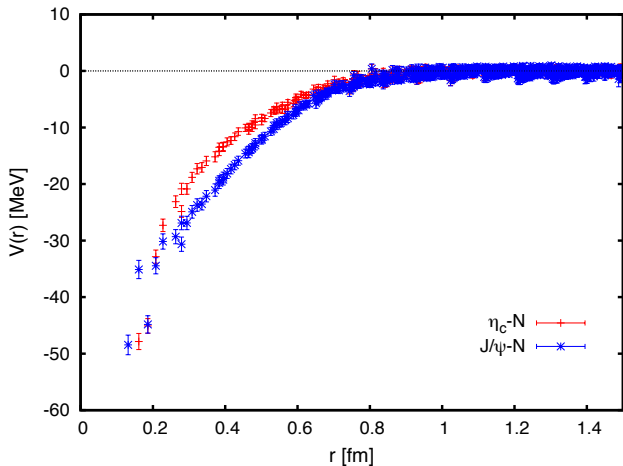


FIG. 3: The central and spin-independent part of the J/ψ - N potential at $M_\pi = 640$ MeV. The η_c - N potential is also included for comparison.

It can be expressed by an orthogonal sum of spin-1/2 and spin-3/2 components [7]: $G_{ij}^{h_1-h_2} = G^{1/2} \mathcal{P}_{ij}^{1/2} + G^{3/2} \mathcal{P}_{ij}^{3/2}$ where proper spin projection operators for the spin-1/2 and spin-3/2 contributions are given by $\mathcal{P}_{ij}^{1/2} = \frac{1}{3} \gamma_i \gamma_j$ and $\mathcal{P}_{ij}^{3/2} = \delta_{ij} - \frac{1}{3} \gamma_i \gamma_j$ in the center of mass frame [22]. Then, each spin part can be projected out as $G^{1/2} = \sum_{i,j} \mathcal{P}_{ij}^{1/2} G_{ji}^{h_1-h_2}$ and $G^{3/2} = \frac{1}{2} \sum_{i,j} \mathcal{P}_{ij}^{3/2} G_{ji}^{h_1-h_2}$ where the indices i and j are also summed over all spatial directions.

As a result, we can obtain the BS wave function and the resulting J/ψ - N potential for each spin channel. Although the lower-spin state (spin-1/2) is not free from the contamination of the η_c - N state through channel mixings [7], we simply consider the spin averaged four-point

correlation function for the J/ψ - N system as

$$G_{\text{ave}}^{J/\psi-N} = \frac{1}{3} G^{1/2} + \frac{2}{3} G^{3/2} = \frac{1}{3} \sum_i G_{ii}^{J/\psi-N}. \quad (5)$$

This procedure may provide only a spin-independent part of the J/ψ - N potential through the same analysis applied to the η_c - N system.

We show our result of the J/ψ - N potential in Fig. 3 where the η_c - N potential is included for comparison. The J/ψ - N potential shows short-range attraction. Similar to what we discussed in the η_c - N case it does not have a normal “van der Waals type” $-1/r^n$ behavior. There is no qualitative difference between the η_c - N and J/ψ - N potentials. Quantitatively, the attractive interaction observed in the J/ψ - N potential is rather stronger than that of the η_c - N system as shown in Fig. 3, though it is still not strong enough to form a bound state in the J/ψ - N system.

What is a possible origin of the stronger attraction appearing in the J/ψ - N system? As was discussed previously, the attractive interaction in the $c\bar{c}$ - N system tends to be slightly stronger as the light quark mass increases. It should be recalled that the reduced mass of the $c\bar{c}$ - N system is also changed through a variation of the light quark mass. Supposed that the strength of the $c\bar{c}$ - N potential depends simply on the reduced mass of the $c\bar{c}$ - N system, a mass difference of the η_c and J/ψ state may account for the difference between the η_c - N and J/ψ - N potentials. However, this is not the case. As shown in the inset of Figure 2, the η_c - N potential gets deeper, when the reduced mass of the η_c - N system is increased by about 10% through a variation of the light quark mass. On the other hand, although the reduced mass receives only about 1% gains in the J/ψ - N system relative to the η_c - N system, the difference between the η_c - N and J/ψ - N potentials shown in Fig. 3 is much bigger than the

reduced mass dependence observed in Fig. 2. This may indicate that the stronger interaction in the J/ψ - N system than in the η_c - N system is caused by some dynamics associated with the structure of quarkonia.

We again recall that the ordinary van der Waals interaction is sensitive to the size of the charge distribution. Therefore, what we observed here is intuitively accounted for by the simple speculation that the size of the J/ψ state is larger than that of the η_c state. Nevertheless, similar to the η_c - N system in the J/ψ - N no appreciable finite-size effects are observed.

We have studied the charmonium-nucleon potential $V_{c\bar{c}N}(r)$ in quenched lattice QCD. Potentials between charmonia (η_c and J/ψ) and the nucleon are calculated from the equal-time BS amplitude through the effective Schrödinger equation. We have found that the central and spin-independent potential $V_{c\bar{c}N}(r)$ in both the η_c - N and J/ψ - N systems is weakly attractive at short distances and exponentially screened at large distances. It is observed that both potentials have no appreciable finite-size dependence and no significantly large quark-mass dependence within the pion mass region $640\text{MeV} \leq M_\pi \leq 870\text{MeV}$. The J/ψ - N system is slightly stronger attractive than the η_c - N system. This should be accounted for by the dynamics associated with the structure of quarkonia.

In order to make a reliable prediction about the nuclear-bound charmonium, an important step in the future is clearly an extension to dynamical lattice QCD simulations in the lighter quark mass region. Such planning is now underway. Once we obtain a realistic potential, we will proceed exploring the nuclear-bound charmonium state with theoretical inputs of the charmonium-nucleon potential by using the exact few-body calculation.

We would like to thank T. Hatsuda for helpful suggestions and fruitful discussions. We also thank to T. Misumi for his careful reading of the manuscript. T.K. is supported by Grant-in-Aid for the Japan Society for Promotion of Science (JSPS) Research Fellows (No. 22-7653). S.S. is supported by the JSPS Grant-in-Aids for Scientific Research (C) (No. 19540265) and Scientific Research on Innovative Areas (No. 21105504). Numerical calculations reported here were carried out on the PACS-CS supercomputer at CCS, University of Tsukuba and also on the T2K supercomputer at ITC, University of Tokyo.

[†] Electronic address: ssasaki@phys.s.u-tokyo.ac.jp

- [1] S. J. Brodsky, I. A. Schmidt and G. F. de Teramond, Phys. Rev. Lett. **64**, 1011 (1990).
- [2] S. J. Brodsky and G. A. Miller, Phys. Lett. B **412**, 125 (1997).
- [3] M. E. Luke, A. V. Manohar and M. J. Savage, Phys. Lett. B **288**, 355 (1992).
- [4] T. Appelquist and W. Fischler, Phys. Lett. B **77**, 405 (1978).
- [5] G. Feinberg and J. Sucher, Phys. Rev. D **20**, 1717 (1979).
- [6] A. Hayashigaki, Prog. Theor. Phys. **101**, 923 (1999).
- [7] K. Yokokawa, S. Sasaki, T. Hatsuda and A. Hayashigaki, Phys. Rev. D **74**, 034504 (2006).
- [8] D. A. Wasson, Phys. Rev. Lett. **67**, 2237 (1991).
- [9] V. B. Belyaev et al., Nucl. Phys. A **780**, 100 (2006).
- [10] N. Ishii, S. Aoki and T. Hatsuda, Phys. Rev. Lett. **99**, 022001 (2007).
- [11] S. Aoki, T. Hatsuda and N. Ishii, Prog. Theor. Phys. **123** (2010) 89.
- [12] M. Lüscher, Nucl. Phys. B **354**, 531 (1991).
- [13] S. Aoki *et al.* [CP-PACS Collaboration], Phys. Rev. D **71**, 094504 (2005).
- [14] R. Sommer, Nucl. Phys. B **411**, 839 (1994) [arXiv:hep-lat/9310022].
- [15] M. Guagnelli, R. Sommer and H. Wittig [ALPHA collaboration], Nucl. Phys. B **535**, 389 (1998); S. Necco and R. Sommer, Nucl. Phys. B **622**, 328 (2002)
- [16] M. Lüscher, S. Sint, R. Sommer, P. Weisz and U. Wolff, Nucl. Phys. B **491**, 323 (1997).
- [17] S. Aoki, Y. Kuramashi and S. I. Tominaga, Prog. Theor. Phys. **109**, 383 (2003).
- [18] A. X. El-Khadra, A. S. Kronfeld and P. B. Mackenzie, Phys. Rev. D **55**, 3933 (1997).
- [19] Y. Kayaba *et al.* [CP-PACS Collaboration], JHEP **0702**, 019 (2007).
- [20] T. T. Takahashi, T. Umeda, T. Onogi and T. Kunihiro, Phys. Rev. D **71**, 114509 (2005) [arXiv:hep-lat/0503019].
- [21] S. Matsuyama and H. Miyazawa, Prog. Theor. Phys. **61**, 942 (1979).
- [22] M. Benmerrouche, R. M. Davidson and N. C. Mukhopadhyay, Phys. Rev. C **39** (1989) 2339.
- [23] T. Yamazaki *et al.*, Phys. Rev. D **79**, 114505 (2009) [arXiv:0904.2039 [hep-lat]].
- [24] M. A. B. Beg and A. Zepeda, Phys. Rev. D **6**, 2912 (1972).
- [25] The potential for $r \gtrsim 2$ fm deviates slightly from zero beyond statistical errors. This should be an artifact of the finite cubic box of $(3.0 \text{ fm})^3$. It is worth noting that the r -dependence of the potential in the region of $r \gtrsim 1.5$ fm is mainly determined by off-axis separations. The difference between on and off-axis separations can be caused by a rotational symmetry breaking in the finite cubic box.

* Electronic address: kawanai@nt.phys.s.u-tokyo.ac.jp